Coexistence of non-Fermi liquid behavior and biquadratic exchange coupling in La-substituted CeGe: Nonlinear susceptibility and DFT+DMFT study

Karan Singh [1], Antik Sihi [1], Sudhir K. Pandey,[2] and K. Mukherjee [1]
[1]*School of Basic Sciences, Indian Institute of Technology Mandi, Mandi 175075, Himachal Pradesh, India*
[2]*School of Engineering, Indian Institute of Technology Mandi, Mandi 175075, Himachal Pradesh, India*

(Received 28 August 2020; revised 12 November 2020; accepted 24 November 2020; published 16 December 2020)

Studies connected with the investigations of "non-Fermi liquid" (NFL) systems continue to attract interest in the condensed-matter physics community. Understanding the anomalous physical properties exhibited by such systems and its related electronic structures is one of the central research topics in this area. In this context, Ce-based and Ce-site diluted (with nonmagnetic ions) compounds provide a fertile playground. Here, we present a detailed study of nonlinear DC susceptibility and combined density-functional theory plus dynamical mean-field theory (DFT+DMFT) on $Ce_{0.24}La_{0.76}Ge$. Theoretical investigation of $4f$ partial density of states, local susceptibility, and self-energy demonstrates the presence of NFL behavior which is associated with fluctuating local moments. Nonlinear DC susceptibility studies on this compound reveal that the transition from NFL state to the new phase is due to development of the biquadratic exchange coupling and it obeys the nonlinear susceptibility scaling. Under the application of magnetic fields, local moments interact spatially through conduction electrons resulting in magnetic fluctuations. Our studies point to the fact that the origin of the observed biquadratic exchange coupling is due to the spatial magnetic fluctuations.

DOI: 10.1103/PhysRevB.102.235137

I. INTRODUCTION

Novel electronic states of strongly correlated electron systems with partially filled f- or d shells continue to evoke interest in the condensed-matter community [1]. In many members of this family, non-Fermi liquid (NFL) phenomenon is often developed in the vicinity of a quantum critical point (QCP). At QCP, magnetic ordering temperature is driven to zero by alloying or by applying pressure or magnetic fields [2,3]. Some of the best-known examples in the correlated f- and d-electrons systems where the NFL behavior is observed are $CeCoIn_5$ [4], $CeCu_{5.1}Au_{0.9}$ [5], $Ce(Ru_{0.5}Rh_{0.5})_2Si_2$ [6], $YbRh_2Si_2$ [7], $UCu_{5-x}Pd_x$ [8], and Ni_xPd_{1-x} [9], etc. The low-temperature physical properties of correlated electron systems usually follow Landau's Fermi liquid (LFL) theory which is based on a paradigm that the T^2 dependence of DC resistivity (ρ) is due to prevailing single transport relaxation rate, which originates from the electron-electron scattering. When the Fermi liquid state becomes unstable, an anomalous state (with ρ varying as T^α, with $\alpha \neq 2$), i.e., the so-called NFL behavior would emerge. Such a behavior arises due to the presence of quantum fluctuations, which are enhanced due to a strong competition between on-site Kondo effect and the intersite Ruderman-Kittel-Kasuya-Yosida (RKKY) interactions. Additionally, some attempts have also been made to explain the NFL behavior based on the possibility of an unconventional Kondo effect [10] or disorder effects [11]. Generally, clean strongly correlated systems are characterized by a large amount of the scattering of the metallic carriers by the localized magnetic moments. When the temperature is lowered, the lattice translation invariance set in and a quick drop of the resistivity occurs below so-called coherence temperature [12]. The dilution of localized magnetic moments by substitution of nonmagnetic ion has led to a single-impurity-like behavior and coherent temperature is affected [13]. Furthermore, it is expected that the interplay of the disorder effect would destroy the lattice translation invariance. Thereby the coherent temperature is suppressed and might lead to the observation of NFL behavior [12,14]. As a result, various anomalous variations of the physical properties are observed due to the presence of different relaxation rates. Hence, it can be said that in the presence of disorder, the interplay of conduction electrons with localized magnetic moments (through Kondo coupling) is affected, which might give rise to the NFL behavior [14]. This mechanism can be understood on the basis that disorder leads to a broad distribution of Kondo temperature. It results in a finite fraction of the unquenched localized moments which resides at all temperatures. This adds an exchange interaction term in the Hamiltonian, which can be due to the randomness in the RKKY intersite coupling [3]. This phenomenon is usually expected in disordered Kondo alloy, where the intersite interaction energy dominates over the Kondo energy associated with magnetic fluctuations [15]. These fluctuations may develop biquadratic exchange coupling at very low temperatures and/or under the application of external magnetic fields [16–18].

In some d-electron systems (like $BaRuO_3$, $SrRuO_3$) exhibiting NFL behavior, the electronic properties have been systematically studied by employing a single-site dynamical mean-field model with rotationally invariant interactions. For such model, Matsubara self-energy [$\mathrm{Im}\sum(i\omega)$] varies as ω^α (where $\omega =$ frequency and exponent $\alpha = 1/2$) [19,20].

McKenzie and Scarratt had reported that the presence of NFL state gives rise to a positive slope in the real part of the self-energy and exhibits a dip in the imaginary part of the self-energy [21]. In the presence of magnetic fields, Fermi liquid behavior can be observed with $\alpha = 1$ [19,20]. In $4f$-electron systems, the density-functional theory plus dynamical mean-field theory (DFT+DMFT) approach has been applied to understand the electronic structure [22,23]. But, to the best of our knowledge, a systematic detailed investigation of electronic structure along with its relationship with the biquadratic exchange coupling is lacking for the $4f$-based NFL systems.

To shed some light on the possible presence of biquadratic exchange coupling, associated with NFL behavior, we choose our recently studied $Ce_{0.24}La_{0.76}Ge$ compound [24]. The corresponding parent compound, CeGe, undergoes antiferromagnetic-type transition along with development of multipolar moments around 10.7 K. In the presence of magnetic fields, long-ranged antiferromagnetic order is preserved. The Sommerfeld coefficient of this compound is found to be $\sim 0.267\,\mathrm{J/mol\,K^2}$ [25]. This suggests an increase in the mass of electrons by partial screening of $4f$ moments through the conduction electrons. Hence, this compound can be considered in the category of disordered Kondo system. The above statement can be made on the basis of the fact that the Kondo peak in resistivity is absent [25–28]. This observation is ascribed to the dominating intersite interactions energy, which impedes the whole screening of magnetic moments. Due to the substitution of La, disorder-driven NFL behavior is observed in $Ce_{0.24}La_{0.76}Ge$ [24]. Interestingly, in this compound, in the presence of magnetic fields, an anomaly [above $2(10^4)$ Oe] in heat capacity, is noted over a wide temperature range. The peak got shifted to higher temperatures with increasing fields [24]. Thus, in this compound a changeover from NFL state to a new phase is noted. These observations raise the following questions: (1) whether the NFL state is associated with the local moment fluctuations? (2) whether the observed new phase is due to the presence of biquadratic exchange coupling? and (3) If yes, is the biquadratic exchange coupling related to fluctuations?

In order to address these queries, in this paper we present a detailed study of nonlinear DC susceptibility and combined density-functional theory plus dynamical mean-field theory on $Ce_{0.24}La_{0.76}Ge$. Nonlinear DC susceptibility provides an ideal method to test the equilibrium nature of a phase transition involving higher-order exchange interaction terms. The scaling of nonlinear susceptibility is a signature of the genuine existence of equilibrium phase transition where static critical exponents are found and they are related to each other through hyperscaling relation [29–31]. A reliable explanation about the NFL behavior can be given, with the aid of DFT+DMFT calculations [32]. This approach solves the localized impurity problem at finite temperature, in which the self-energy is the function of ω only. It also describes the localization effect and quasiparticle excitations [32,33]. Additionally, to support computational methods, parameters adopted, and the obtained results for this compound, we will also discuss the computational result of the parent CeGe.

Our results indicate that in $Ce_{0.24}La_{0.76}Ge$, nonlinear DC susceptibility scaling is satisfied. The scaling suggests that transition from the NFL to a new phase is due to development of the biquadratic exchange coupling in the presence of magnetic fields. In zero magnetic field, theoretical results also indicate to the presence of NFL state which is associated with local moment fluctuations. These observations can be attributed to the fact that the local moments interact spatially through conduction electrons in the presence of magnetic fields. It results in the development of spatial magnetic fluctuations which is associated with the biquadratic exchange coupling. Thus, it can be said that this field-induced phase is derived from the spatial magnetic fluctuations.

II. METHODS

The compounds CeGe and $Ce_{0.24}La_{0.76}Ge$ are the same as those reported in Refs. [24,25]. Nonlinear susceptibility measurements are performed using Magnetic Property Measurement System from Quantum Design, USA. For computational studies, we used dynamical mean-field theory on top of density-functional theory. In recent years, the DFT+DMFT is one of the most advanced electronic structure methods for investigations of strongly correlated electron systems. In this study, the spin-orbit coupled calculations are performed for these compounds with the help of full-potential linearized-augmented plane-wave method as implemented in WIEN2K code [34]. The local density approximation is chosen as the exchange-correlation functional for these calculations [35]. The DFT+DMFT calculations are done using EDMFT [32] code, where the DFT part is carried out using WIEN2K code [34]. In this scenario, the Hubbard $U = 6.0\,\mathrm{eV}$ and Hund's coupling $J = 0.7\,\mathrm{eV}$ are fixed to solve the impurity problem using continuous-time quantum Monte Carlo method [36]. Here, "nominal" method is selected to take care of the double-counting problem [37]. To transfer the spectral function from imaginary to real axis, maximum entropy analytical continuation method is employed [38]. 160 k points in irreducible Brillouin zone is the set for this study. It is to be noted that both these compounds crystallize in the orthorhombic structure with *Pnma* space group. The lattice parameters used for the calculation are extracted from the Rietveld refinement of the x-ray-diffraction pattern. At this point, it is to be mentioned that virtual crystal approximations [39] are chosen to study the effect of La doped on the correlated Ce $4f$ electrons.

III. RESULTS

A. Nonlinear susceptibility study

The nonlinear susceptibility is expressed as [18,40]

$$M/H = \chi_0 - \chi_1 H^{a(T)-1}, \tag{1}$$

where χ_0 is the linear magnetic susceptibility and χ_1 is a nonlinear magnetic susceptibility term. $a(T)$ is the exponent determined at different temperatures. In $Ce_{0.24}La_{0.76}Ge$, in order to investigate the possibility of the presence of higher-order magnetization, the nonlinear DC susceptibility is studied. This study is useful for the determination of high-order susceptibility terms which are dependent on very low frequencies (less than 10^{-2} Hz) and are generally hidden in direct AC susceptibility measurements. The nonlinear parts of DC susceptibilities are obtained from field and temperature dependence of magnetization (see Fig. S1 of Supplemental

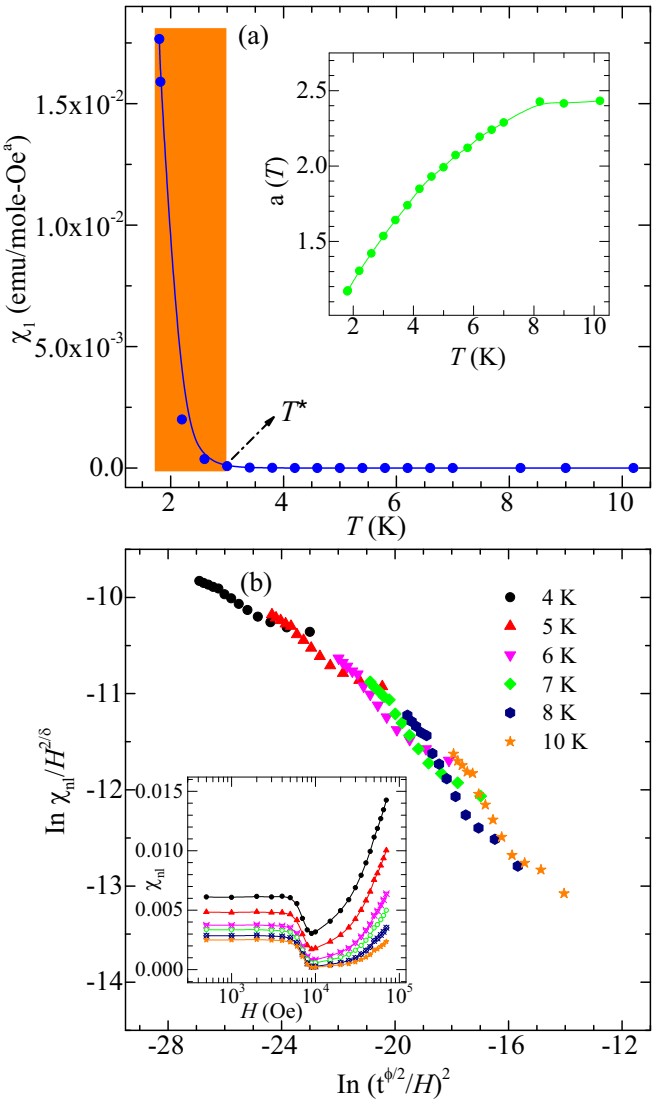

FIG. 1. (a) Temperature-dependent χ_1 for $Ce_{0.24}La_{0.76}Ge$. Orange shaded area represents the higher-order susceptibility regime, below temperature T^*. Inset: Exponent $a(T)$ plotted as a function of temperature. (b) Scaling plots of χ_{nl}, above $2(10^4)$ Oe for $Ce_{0.24}La_{0.76}Ge$. Inset: H-dependent χ_{nl} at different temperatures.

Material [41]) using the protocol as given in Refs. [18,40,42]. Figure 1 shows the temperature (T)-dependent χ_1. Interestingly, it is noted that χ_1 grows sharply below T^* (~3 K). This observed feature can be referred to an energy scale (shaded region in Fig. 1) due to the development of higher-order susceptibility in the presence of magnetic fields [18]. The inset of Fig. 1 shows the temperature-dependent exponent $a(T)$. This exponent decreases with decreasing temperature and reaches 1.5 around 3 K. This observed value is not in accordance with the quadrupole picture [$a(T) = 4$], octupole picture [$a(T) = 6$], etc. As mentioned earlier, in the zero-field limit ($H \to 0$), disorders-driven NFL behavior is present in this compound [24]. The variation of linear susceptibility χ_0 (see Fig. S2 of Supplemental Material) indicates that there is the presence of local magnetic moments which increases with decreasing temperature. In the external magnetic fields, these moments are responsible for the development of a phase which is possibly associated with biquadratic exchange coupling. This feature can be clearly seen as an anomaly in heat capacity measurements over a wide temperature range (around T^*), above $2(10^4)$ Oe (see Fig. S3 of Supplemental Material). The inset of Fig. 1(b) shows the total nonlinear susceptibility $\chi_{nl}(\chi_0\text{–}M/H)$ as a function of the magnetic field. In the temperature range 4–10 K, it is noted that χ_{nl} is independent at low fields. Above $1(10^4)$ Oe, it increases nonlinearity and slope of the curve also increases with decreasing temperature. Hence, it might be said that a field-induced biquadratic exchange coupling possibly leads to the development of the higher-order magnetization.

To investigate the equilibrium nature of phase transition associated with biquadratic exchange coupling, we relate this coupling to the spin freezing which leads to the divergence of the so-called spin glass susceptibility χ_{SG} [43],

$$\chi_{nl} = \beta^3(\chi_{SG}\text{–}2/3), \tag{2}$$

where β is critical exponent associated with an order parameter q. This order parameter q is proportional to t^β [$t = (T/T^* - 1)$ is the reduced temperature]. χ_{SG} is defined as [43]

$$\chi_{SG} = \beta^2[(\langle S_iS_j\rangle - \langle S_i\rangle\langle S_j\rangle)^2]_{av}, \tag{3}$$

where $\langle\ldots\rangle$ and $[\ldots]$ denote the thermal averages and an average over the disorders, respectively; S_i and S_j are the magnetic moment at site i and j, respectively. Further, the most relevant test for ascribing the critical behavior of the phase transition can be extracted by the scaling of χ_{nl}. In our case, it is anticipated that χ_{nl} (T^*,H) begins to diverge around temperature T^* or below (where χ_0 is nondivergent) with the power law as $\chi_{nl}(T^*, H) \propto H^{2/\delta}$ and $t^{-\gamma}$ (δ and γ are critical exponents that are related with β). A scaling form of χ_{nl} is defined as [40,43]

$$\chi_{nl}(T^*, H) = H^{2/\delta} f(t/H^{2/\varphi}), \tag{4}$$

where $\varphi = \beta + \gamma$, $\delta = (\beta + \gamma)/\beta$, and $f(x)$ is an arbitrary scaling function and follows the asymptotic behavior; $f(x) =$ const, $x \to 0$, and $f(x) = x^{-\alpha}$, $x \to \infty$. The exponents δ and φ can be determined through scaling. Figure 1(b) shows the scaling of χ_{nl} ($T\chi_{nl}$,H) with parameters $T^* = 3$ K, $\delta = 5 \pm 0.3$, and $\varphi = 4 \pm 0.1$, above $2(10^4)$ Oe. Using the relation $\varphi = \beta + \gamma$ and $\delta = (\beta + \gamma)/\beta$, the γ is equals to $\varphi(\delta\text{–}1)/\delta$ and has a value of 3.2. A similar type of scaling and critical exponents has been reported for the GdAl system [18]. The critical exponent $\beta(= \varphi/\delta)$ associated with order parameter q is equal to 0.8 and determines the exponent ν of the correlation length $\xi(\propto t^{-\nu})$ from the relation $d\nu = 2\beta + \gamma$ (d = dimensionality) [44]. For $d = 3$, ν equals to 1.6, and this value suggests that the order parameter can develop a spin-freezing-like transition when biquadratic exchange coupling associated with squared correlation function $(S_iS_j)^2$ turns into long-range ordering [43]. Hence, it can be said that the field-induced phase originates due to establishment of partial order parameter associated with biquadratic exchange coupling (further discussed in Sec. IV). In the next section, we perform DFT+DMFT calculations for this compound to get a deeper insight about the NFL state.

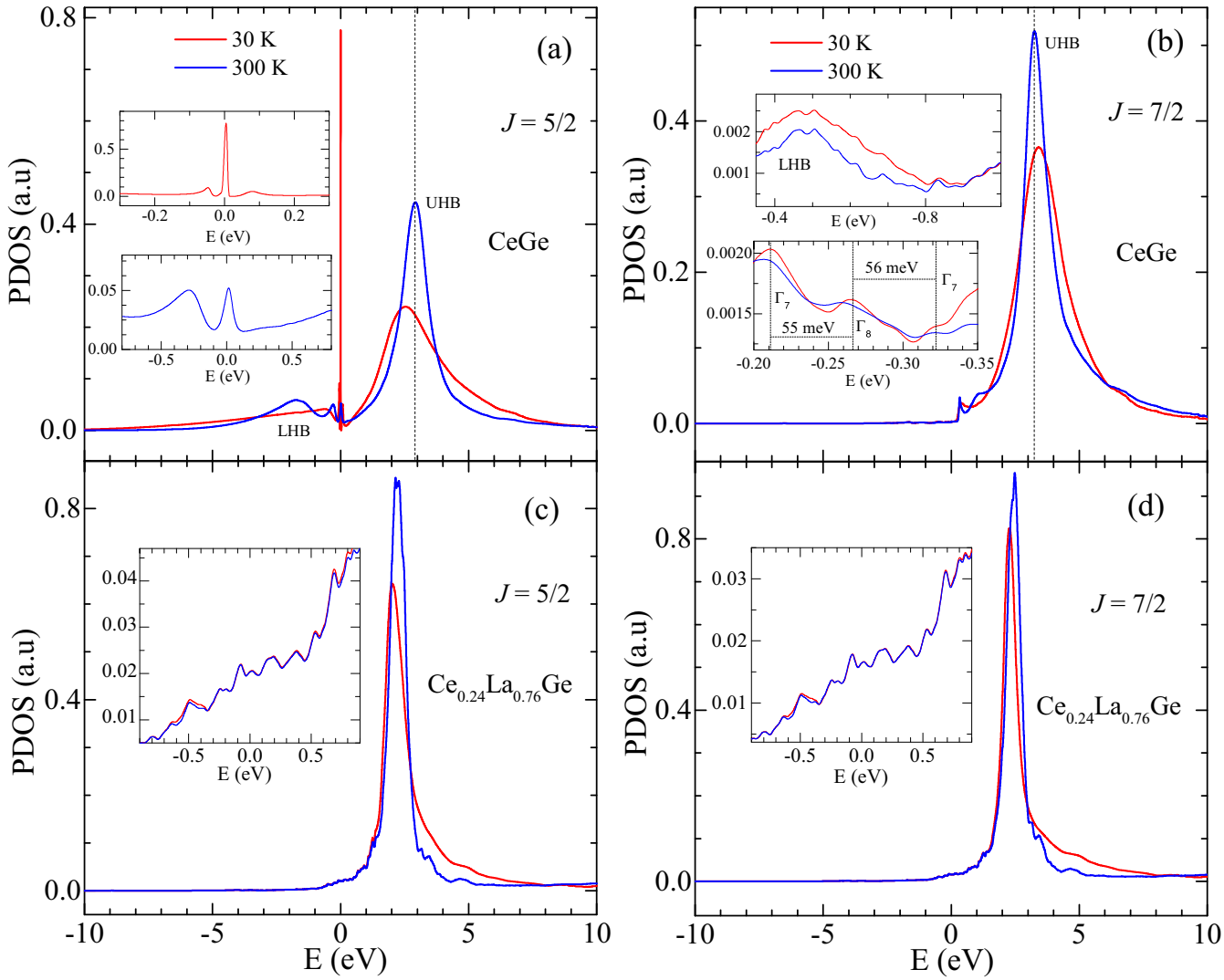

FIG. 2. PDOS of Ce $4f$ at 30 and 300 K: (a), (b) for CeGe; (c), (d) for $Ce_{0.24}La_{0.76}Ge$. Upper and lower inset of (a) shows the PDOS around Fermi level at 30 and 300 K, respectively. Upper and lower inset of (b) shows the PDOS at low negative energy at both 30 and 300 K. Inset of (c) and (d) shows the PDOS around Fermi level. Zero energy corresponds to the Fermi level. LHB is the lower Hubbard band and UHB is the upper Hubbard band.

B. Computational study using DFT+DMFT

1. Density of states and susceptibility

DFT in combination with the DMFT can be used to capture the evolution of NFL state arising from $4f$-electron configurations under finite temperatures [21,22,32]. In this subsection, we will focus on the computational results for CeGe and $Ce_{0.24}Ce_{0.76}Ge$. For CeGe, Figs. 2(a) and 2(b) show the partial density of states (PDOS) for $J = 5/2$ and $J = 7/2$ subbands of Ce $4f$ in energy window -10 to 10 eV, respectively. Ce $4f$ orbitals are split into the $J = 5/2$ and $J = 7/2$ subbands, which is induced by the spin-orbit coupling. In both cases, a large peak is observed at 2.90 eV (for $J = 5/2$) and 3.17 eV (for $J = 7/2$), which can be assigned to the upper Hubbard bands [23,32]. These observed peaks can arise due to the localized $4f$ electrons. The distance between two peaks is about 270 meV, which is close to the reported value of spin-orbit splitting $\Delta_{SO} = 280$ meV [45]. A weak lower Hubbard band is also observed at the -1.7 eV [Fig. 2(a)] and -0.5 eV [upper inset of Fig. 2(b)] for $J = 5/2$ and $J = 7/2$, respectively. This observed upper and lower Hubbard band arises due to the effective on-site Coulomb potential (U_{eff}). At low temperatures (around 30 K), similar upper Hubbard band with a shift in energy is seen, for both $J = 5/2$ and $J = 7/2$, but, the intensity of the peak is smaller. The lower Hubbard band disappears for $J = 5/2$, but, interestingly, a quasiparticle peak appears in the vicinity of Fermi level [see upper inset of Fig. 2(a)]. This means that U_{eff} is reduced due to partial screening of the $4f$ electrons. With decreasing temperatures, magnetic moments combine with conduction bands to form a heavy quasiparticle fluid, having a mass which is very large compared to the mass of free electrons. This forms a quasiparticle peak in the vicinity of Fermi level in Ce-$4f$ PDOS. On the other hand, it reduces the weight of the upper Hubbard band and the weaker lower Hubbard band is suppressed. This indicates that $J = 5/2$ subband could be the source of the effective mass. A similar feature was also noted in other Ce-based compound like $CeRu_2Si_2$ [23]. Mostly, quasiparticles form the Fermi

liquid state which has a mean-free path much larger than their wavelength [46]. For this state, resistivity varies quadratically at low temperature and self-energy $\Sigma(\omega)$ varies as ω^2 [47]. For CeGe, quadratic variation of resistivity has not been observed [25], suggesting that the mean-free path might be smaller than its wavelength. The quasiparticle picture is not seen for the $J = 7/2$ subband, but we see the three peaks in the energy window -0.2 to -0.35 eV [lower inset of Fig. 2(b)]. In this energy window, the $J = 5/2$ and $J = 7/2$ subbands can be further split into doublet (Γ_7) and quartet state (Γ_8) under crystalline electric-field effects [48–50]. The $J = 5/2$ splits into ground state Γ_8 and excited state Γ_7 where $J = 7/2$ splits into ground state Γ_7 and two excited states Γ_8 and Γ_7. The lower inset of Fig. 2(a) shows a peak in the energy window -0.2 to -0.35 eV, indicating that there might be absence of quartet state for 5/2 subbands. But, for $J = 7/2$, three peaks are observed in this energy window, indicating the presence of the quartet state. The distance between the ground state Γ_7 and first excited state Γ_8 and the distance between the first excited state Γ_8 and second excited state Γ_7 are 55 and 56 meV, respectively. The observed energy difference between Γ_7 and Γ_8 is close to the 50 meV which has been reported in other Ce-based compound, e.g.. CeB_6 [49,51]. The quartet state usually produces multipolar moments that have also been reported experimentally for CeGe [25].

Figures 2(c) and 2(d) show the plot of the PDOS in the energy window -10 to 10 eV at 30 and 300 K for the $J = 5/2$ and $J = 7/2$ subbands, respectively, of $Ce_{0.24}La_{0.76}Ge$ compound. It is noted that both subbands behavior is similar. But, one large peak at 2.39 eV (away from the Fermi level) is observed. With decreasing temperature (30 K), this peak becomes somewhat smaller and broader. Hence, it can be said that the localized nature $4f$ electrons (as appeared in CeGe) preserve in the $Ce_{0.24}La_{0.76}Ge$. The quasiparticle picture is not observed at the Fermi level in the $Ce_{0.24}La_{0.76}Ge$ compound [inset of Figs. 2(c) and 2(d)]. It can be due to the presence of NFL state [24]. Hence, it can be said that dynamical screening effect is not important in this compound which possibly evades the quasiparticle picture. In Refs. [52,53] it has been discussed that the quasiparticle is suppressed in the NFL paradigm and some local moments are preserved. Within the framework of DFT+DMFT we can compute the local spin susceptibility $\chi_{\rm loc}$ for both compounds [54–56]

$$\chi_{\rm loc} = \int_0^\beta d\tau [\langle S_i(\tau) S_i(0)\rangle], \tag{5}$$

where β is the inverse temperature. The operator $S_i = (1/2M)\sum_{\gamma=1}^{M}(c^\dagger_{i\gamma\uparrow}c_{i\gamma\uparrow} - c^\dagger_{i\gamma\downarrow}c_{i\gamma\downarrow})$, M indicates the number of f orbitals, i is the site index, and γ is the orbital index. The operator $c_{i\gamma\uparrow}(c^\dagger_{i\gamma\uparrow})$ is the annihilator (creator) of the electron. $\langle S_i(\tau)S_i(0)\rangle$ is the imaginary time-dependent spin-spin correlation function. At high temperatures, $\chi_{\rm loc}$ follow the behavior as $\chi_{\rm loc} = C/T$ (where C = Curie constant) [56]. Figure 3 shows the temperature-dependent ${\chi_{\rm loc}}^{-1}$ for CeGe. The fitted $\chi_{\rm loc}$ gives $C[\sim \langle S_i(\tau)S_i(0)\rangle]$ equal to 0.92. This implies that the $4f$ electron sustains the local nature of the magnetic moments and the spins at different τ points are correlated. The effective local magnetic moment $\mu_{\rm eff}$ is also calculated using the relation $2.827\sqrt{C}\,\mu_B$, which is around

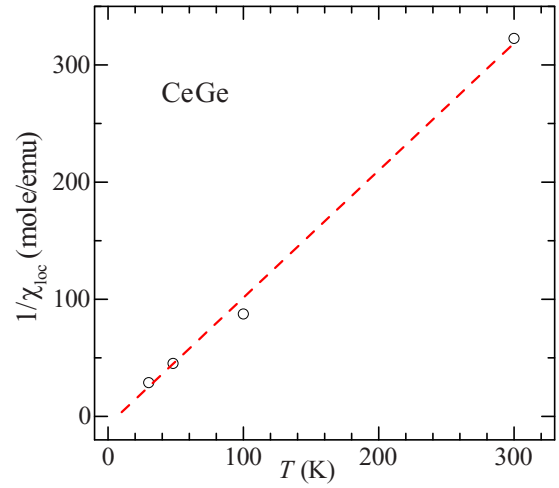

FIG. 3. Temperature-dependent inverse local spin susceptibility ($1/\chi_{\rm loc}$) for CeGe. Red line through the data points indicates the linear fitting.

2.71 μ_B. This value is close to the expected value of 2.52 $\mu_{\rm B}$, calculated using the formula $\mu_{\rm eff} = g_J\sqrt{J\,(J+1)}\,\mu_B$, where $J = 5/2$, $g_J = 6/7$, and reported experimental value ($\sim$ 2.4 μ_B) for this compound [25]. For $Ce_{0.24}La_{0.76}Ge$, the computed $\chi_{\rm loc}$ does not vary significantly with temperature. This might be due to trivial presence of the spin-spin correlations $\langle S_i(\tau)S_i(0)$. This suggests that local moment fluctuations are large, implying that spins at different τ points do not show temperature-dependent correlations. As observed experimentally, temperature-dependence data indicate the presence of the spin-spin correlations in this compound which is significantly weaker in comparison to CeGe. This suggests that virtual crystal approximation is unable to capture spin-spin correlations exactly. Moreover, experimental data also suggest the nonlocal spin-spin interactions. Even though single-site DMFT gives the direct information about the local interactions, however, one expects that hybridization function may contain indirect information about the nonlocal spin-spin interactions when calculations will be performed on the structure with two or more than two inequivalent impurity sites containing Ce atoms. In order to observe the correlation effect via impurity hybridization function for $Ce_{0.24}La_{0.76}Ge$, we performed the calculations on two structures. The unit cell of the first structure (structure 1) is the same as the conventional unit cell. In structure 1, out of four Ce sites the three sites are replaced by the La atoms. In the second structure (structure 2), the volume of the unit cell is twice the volume of the conventional unit cell and there are eight Ce sites; six of Ce sites are replaced by La atoms. Structure 1 and structure 2 give rise to $Ce_{0.25}La_{0.75}Ge$. On these structures, three calculations are performed at temperatures 50, 100, and 300 K. The imaginary part of the impurity hybridization function [$\mathrm{Im}\Delta(i\omega)$] corresponding to these two structures are found to be different at the respective temperatures. We have estimated the difference between imaginary parts of the hybridization functions for these two structures [i.e., $\delta\mathrm{Im}\Delta(i\omega) = \mathrm{Im}\Delta(i\omega)_{\rm structure\,2} - \mathrm{Im}\Delta(i\omega)_{\rm structure\,1}$] and plotted $-\delta\mathrm{Im}\Delta(i\omega)$ as a function of frequency (ω) at 50, 100, and 300 K for $J = 5/2$ (Fig. S4 of

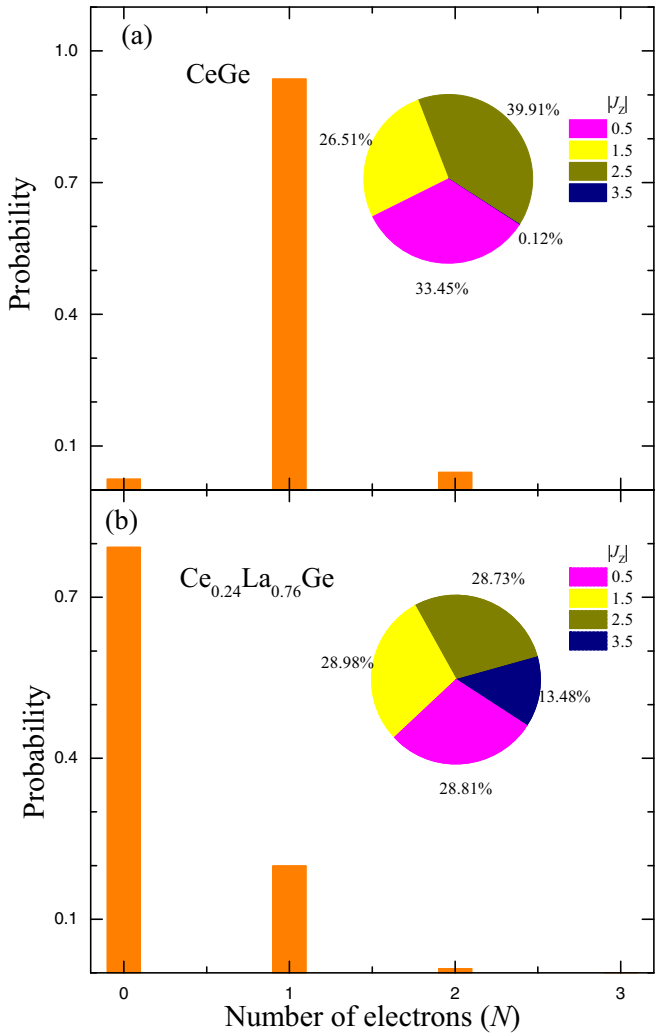

FIG. 4. Probability of N electrons in $4f$ orbitals at 30 K for (a) CeGe and (b) $Ce_{0.24}La_{0.76}Ge$. Inset of (a) and (b) shows the pie-chart, indicating probability of finding the electron in J_z states at 30 K for CeGe and $Ce_{0.24}La_{0.76}Ge$, respectively.

the Supplemental Material). The observed $-\delta \mathrm{Im}\Delta(i\omega)$ may be considered as an evidence of the spin-spin correlation present in the compound. With decreasing temperature, $-\delta \mathrm{Im}\Delta(i\omega)$ increases. This indicates an increase in spin-spin correlations, which is as per our experimental observation.

Figures 4(a) and 4(b) show the probability of finding $4f$ electrons in the electronic configuration N at temperature 30 K for CeGe and $Ce_{0.24}La_{0.76}Ge$, respectively. For CeGe, it is observed that the most probable electronic configuration is $4f^1$ ($N = 1$) having a probability value of 0.935. The probabilities for the $4f^0(N = 0)$, $4f^2(N = 2)$, and $4f^3(N = 3)$ are the 0.024, 0.039, and 3.04×10^{-4}, respectively. This observation suggests that the $4f$ electrons are localized and the mixed valence states are almost absent. For $Ce_{0.24}La_{0.76}Ge$, we find the probabilities 0.793 and 0.19 for $4f^0$ and $4f^1$, respectively. With the introduction of La, the probability of finding electrons in $4f^1$ configuration is reduced and that in $4f^0$ configuration is increased. It indicates that $4f$ electrons favor to stay in a mixed valence state in $Ce_{0.24}La_{0.76}Ge$. In order to see the effect of the spin fluctuations, we plot the pie-chart, which shows the probability for the J_z state [inset of Figs. 4(a) and 4(b)] for CeGe and $Ce_{0.24}La_{0.76}Ge$, respectively. For $|J_z| = 0.5$, 1.5, 2.5, and 3.5, probability of 33.45, 26.51, 39.91, and 0.12% are found for CeGe, whereas the respective probabilities are 28.81, 28.98, 28.73, and 13.48% for $Ce_{0.24}La_{0.76}Ge$. This shows a presence of strong spin fluctuations in both compounds. In CeGe, the spin fluctuations refer to the fluctuations of the magnetic moments which are in localized state and form the magnetic ordering through conduction electrons [25]. In the case of $Ce_{0.24}La_{0.76}Ge$, the probability of finding electrons in $4f$ orbitals is around 0.19. In this compound, the magnetic ordering was also not observed [24]. Hence, in this scenario it appears that the $4f$ electrons present in the localized state fluctuates. This fluctuation may give rise to NFL state as observed experimentally. The presence of NFL state in this compound can be verified through studying the behavior of self-energy at around the Fermi level [21,23].

2. *Self-energy*

We introduce the Green function of the DMFT approximation in terms of self-energy $\Sigma(\omega)$ [47],

$$\mathcal{G}(\omega) = \frac{1}{\omega - \varepsilon_0 - \sum(\omega)}. \tag{6}$$

$\Sigma(\omega)$ contains the real part of self-energy $\mathrm{Re}\Sigma(\omega)$ and imaginary part of self-energy $\mathrm{Im}\Sigma(\omega)$. For noninteracting systems the pole is $\omega = \varepsilon_0$. This is modified to $\omega - \varepsilon_0 - \mathrm{Re}\sum(\omega)$ by electron-electron interactions. For Fermi liquids, in the vicinity of $\omega = 0$ (Fermi level), the real and imaginary self-energy can be expanded as [47]

$$\mathrm{Re}\sum(\omega) \sim -\omega + \text{constant}, \tag{7}$$

$$\mathrm{Im}\sum(\omega) \sim -\omega^2. \tag{8}$$

$\mathrm{Re}\Sigma(\omega)$ gives rise to a negative slope whereas $\mathrm{Im}\Sigma(\omega)$ has a maximum in the vicinity of Fermi level, which can be derived, respectively, from Eqs. (7) and (8). For CeGe, Figs. 5(a) and 5(b) show the Re and $\mathrm{Im}\Sigma(\omega)$ at temperature 30 and 100 K, respectively, for $J = 5/2$ of CeGe. It is noted that $\mathrm{Re}\Sigma(\omega)$ gives rise to negative slope and $\mathrm{Im}\Sigma(\omega)$ has the dip at around Fermi level at 30 K. Similar feature has also been reported for α- and γ-Ce [22]. The lifetime of the quasiparticle depends on $\mathrm{Im}\Sigma(0)$. In the PDOS results, the quasiparticle picture appears in this compound in the vicinity of the Fermi level. In case of Fermi liquids, the lifetime of quasiparticles is infinite at the Fermi level [47]. For CeGe, the value of $Z_k|\mathrm{Im}\sum(0)|$ [where Z_k is the renormalization factor and depends on the effective mass (m^*) such as $1/Z_k \sim m^*$] is around 1.2 meV, suggesting that it has a finite scattering among quasiparticles at Fermi level. As a consequence, it is supposed that the nature of $4f$ electrons may not resemble that of the Fermi liquid behavior in this compound. In Ref. [25], a temperature-dependent resistivity has been reported experimentally for this compound which shows the metallic behavior deviated from description of the Fermi liquid theory

For $Ce_{0.24}La_{0.76}Ge$, Figs. 5(c) and 5(d) represent the $\mathrm{Re}\Sigma(\omega)$ and $\mathrm{Im}\Sigma(\omega)$ at temperature 15, 30, and 100 K, re-

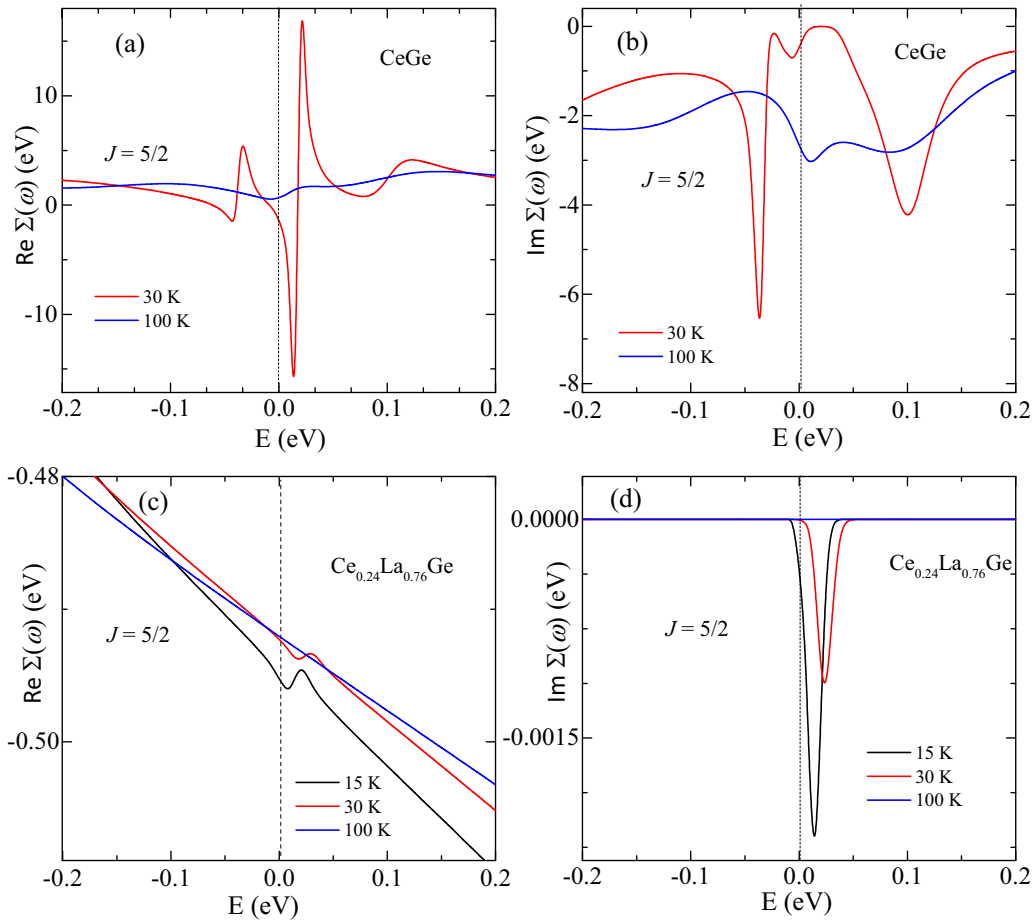

FIG. 5. (a), (b) Real and imaginary part of self-energy for $J = 5/2$ at 30 and 100 K for CeGe. (c), (d) Real and imaginary part of self-energy at 15, 30, and 100 K for $Ce_{0.24}La_{0.76}Ge$. Zero energy corresponds to the Fermi level.

spectively, for $J = 5/2$. At 30 K, it is observed that $\mathrm{Re}\Sigma(\omega)$ exhibits a positive slope at about 0.024 eV where $\mathrm{Im}\Sigma(\omega)$ has a dip. This observed feature shows a shift towards the Fermi level at 15 K. Hence, it is expected that, as the temperature is further decreased, the positive slope in $\mathrm{Re}\Sigma(\omega)$ and the dip in $\mathrm{Im}\Sigma(\omega)$ may move more towards the Fermi level and finally it may arise at the Fermi level at lower temperature. However, in our case, calculations are hard to run below 15 K due to computational limits. This observed behavior is opposite to that reported for the Fermi fluid theory, in both Re and $\mathrm{Im}\Sigma(\omega)$. Also, the quasiparticle peak is not observed in PDOS results. Hence, based on the above observations it can be concluded that there is a presence of NFL state in $Ce_{0.24}La_{0.76}Ge$, which is also in accordance with our experimental reports [24]. We would also like to mention that similar theoretical investigations about NFL state have also been carried out in Ref. [21].

Further to see the implications of the development of the NFL state in $Ce_{0.24}La_{0.76}Ge$, it is useful to introduce Matsubara self-energy, in which all interaction effects are squeezed. Moreover, Matsubara self-energy does not carry the errors arising due to the use of maximum entropy method for analytical continuation of self-energy from imaginary to real frequency. In the NFL state, quantum fluctuations mediate the fermionic-fermionic interactions, which yield a Matsubara self-energy $\mathrm{Im}\sum(\omega) \propto \omega^{\alpha}$ with $\alpha < 1$ [19,20]. Matsubara self-energy can be obtained from the interacting Green's function [47]:

$$\mathcal{G} = \frac{1}{i\omega - \varepsilon_0(k) - \sum(i\omega)}. \tag{9}$$

In this equation, the imaginary part of Matsubara self-energy $\sum(i\omega)$ varies as [19,20]

$$\mathrm{Im}\sum(i\omega) = A(i\omega)^{\alpha} + \gamma. \tag{10}$$

In Refs. [19,20,23] it has been reported that $\mathrm{Im}\sum(i\omega)$ should exhibit a linear behavior at low energy for Fermi liquids and intercept γ is related to the quasiparticle mass enhancement. In Fig. 6, we have plotted ω-dependent $-\mathrm{Im}\sum(i\omega)$ and we observe $\alpha = 0.42$ for $J = 5/2$. This nonlinear ω dependence of the $-\mathrm{Im}\sum(i\omega)$ implies the existence of the NFL state which is in analogy with the above results discussed for this compound.

Finally, based on the self-energy data, the effective mass m^* can be estimated from the equations [46]

$$m^* = m_e\left(1 - \frac{\delta \mathrm{Re}\sum(\omega)}{\delta\omega}\right)\Bigg|_{\omega=0}, \tag{11}$$

where m_e is the mass of the noninteracting band electron. For CeGe, the theoretically calculated effective mass is $\sim 374\, m_e$ for $J = 5/2$ and $\sim 1.54\, m_e$ for $J = 7/2$, at 30 K (see

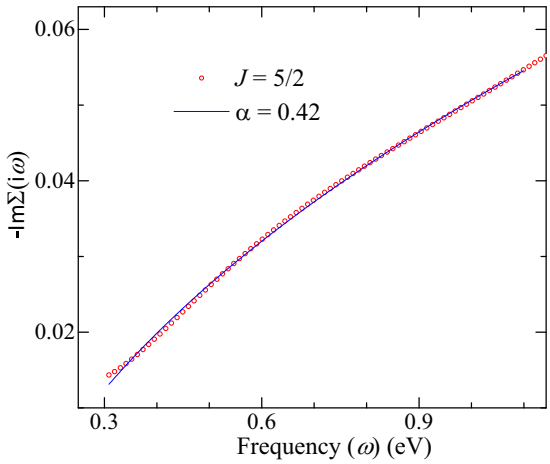

FIG. 6. Imaginary part of the Matsubara self-energy function $\sum(i\omega)$ for $J = 5/2$ at 20 K for $Ce_{0.24}La_{0.76}Ge$. The solid line indicates the fitting using Eq. (10).

Fig. S5 of Supplemental Material [41] information where temperature dependence of m^* is plotted). For $J = 5/2$, the calculated effective mass is closer to the experimental value ($\sim 452\, m_e$, which is calculated from Sommerfeld coefficient $\gamma = 433\,\mathrm{mJ/mol\,K^2}$ [25]), suggesting that large value of γ arises from the $J = 5/2$ subbands. For $Ce_{0.24}La_{0.76}Ge$, the observed values of the m^* for the $J = 5/2$ is about $1.06\, m_e$, at 30 K (see inset of Fig. S5 of Supplemental Material). For $J = 7/2$, the value of m^* is similar, which is around $1.08\, m_e$ at 30 K. It suggests that effective mass is orbital independent in this compound which might be due to the small contributions of $4f$ electrons as a result of 76% La at Ce site. However, this theoretical value is close to the obtained experimental value of $3.87\, m_e$, which is derived from γ ($= 2.43\,\mathrm{mJ/mol\,K^2}$ taken from Ref. [24]).

IV. DISCUSSION

In this section, we attempt to explain the biquadratic exchange coupling through the Heisenberg model in $Ce_{0.24}La_{0.76}Ge$. But before that, we first try to understand the model for magnetic state of the CeGe whose structure is similar to $Ce_{0.24}La_{0.76}Ge$ compound. CeGe crystallizes in the orthorhombic structure with space group *Pnma*, which contains four Ce sites per unit cell. In this structure, the Ge atom is located in a triangular prism of the Ce atoms (see Fig. S6 of Supplemental Material). The structure is similar to FeB-type structure [57]. In each Ce atom, $4f$ shell with one electron (Ce^{3+}) have $S = 1/2$, $L = 3$, $J = |L \pm S| = 5/2$, 7/2 (e.g., ↑, 0, 0, 0, 0, 0, 0). At low temperatures, it is expected that Ce^{3+} multiplet $4f^1$ is separated into a doublet and a quartet state, instead of three doublets, under the influence of the crystalline electric field (CEF) [25,48]. The quartet state has been observed in other Ce-based compound, e.g. CeB_6, in their high-symmetry cubic crystal field [49,51,58]. In the low-symmetry structure, e.g., orthorhombic structure, it has been discussed that weak CEF effect can be responsible for the presence of quartet state [48]. Similarly, the weak CEF, as pointed out, seems to be the most probable cause for the presence of quartet state in the case of the CeGe. As a result in this compound, Ce-$4f$ electrons undergo two ordering phenomena, one driven by dipole-dipole interactions and the other by interactions between multipolar moments [25]. To understand the possible mechanism we write the Heisenberg model, in ordered state, for this compound [59–61]:

$$H = \sum_{i,\ \delta_n} \{J_n S_i S_j + K_n (S_i S_j)^2\}, \tag{12}$$

where $j = i + \delta_n$ (δ_n connects site i and its n th nearest-neighbor sites). J_n and K_n are the bilinear and biquadratic couplings between the n th nearest-neighbor spins, respectively. These couplings undergo the sharp magnetic transition, as seen in temperature response of magnetic susceptibility and heat capacity measurements [25]. This suggests that n should be greater than 1. In experimental study, the results are reported for polycrystalline sample; therefore, we limit our consideration to isotropic bilinear and biquadratic exchange terms. The biquadratic exchange term can be expressed as (which has been proposed for local effective magnetic moment $S \geqslant 1$) [59–61]

$$(S_i S_j)^2 = 1/2 Q_i Q_j - 1/2 S_i S_j + 1/3 S_i^2 S_j^2, \tag{13}$$

where Q_i and Q_j are the quadrupolar moment at site i and j, respectively. By inserting Eq. (13) into (12), Eq. (12) can be rearranged as

$$H = \sum_{i,\ \delta_n} \left\{ (J_n - K_n/2) S_i S_j + K_n \left(1/2 Q_i Q_j + 1/3 S_i^2 S_j^2\right) \right\}. \tag{14}$$

Introduction of La at the Ce site of CeGe suppresses magnetic ordering and develops NFL state in $Ce_{0.24}La_{0.76}Ge$ compound [24]. NFL state is successfully described by DFT+DMFT method. The results of DFT+DMFT calculations are similar to the physics of analytically solvable Sachdev-Ye model. Also according to this model, in NFL state Matsubara self-energy varies as $\sqrt{\omega}$ [62,63]. It is implied that such an NFL state is possible due to strong local moment fluctuations from unquenched magnetic moments. In this work our theoretical studies on $Ce_{0.24}La_{0.76}Ge$ show the presence of the NFL state associated with local moment fluctuations. This is because La substitution can perturb the crystal-field environment which in turn modifies the CEF states (splitting energy and level scheme). Therefore, in $Ce_{0.24}La_{0.76}Ge$, it is expected that the quartet state is destroyed or degeneracy is lifted. The NFL state may originate from the fluctuating nearest-neighbor moment ($n = 1$), where K_n and J_n are supposed to be weak. Interestingly, nonlinear susceptibility scaling suggests a transition from NFL state to a partial order parameter (associated with biquadratic exchange coupling) in the presence of external magnetic fields. To explain such behavior, we take the idea from the reports of Slonczewski *et al.* [16] and Vlasko-Vlasov *et al.* [17], which suggests that magnetic fluctuations can be responsible for the development of field-induced biquadratic exchange coupling. Similarly, in our case, we can state that local moments interact spatially through conduction bands in the presence of magnetic fields resulting in magnetic fluctuations. From Eq. (14), we can understand that K_n is expected to play an important role in the presence of magnetic fields. This leads to the development of the biquadratic exchange coupling in $Ce_{0.24}La_{0.76}Ge$. As a result, a partial order parameter grows

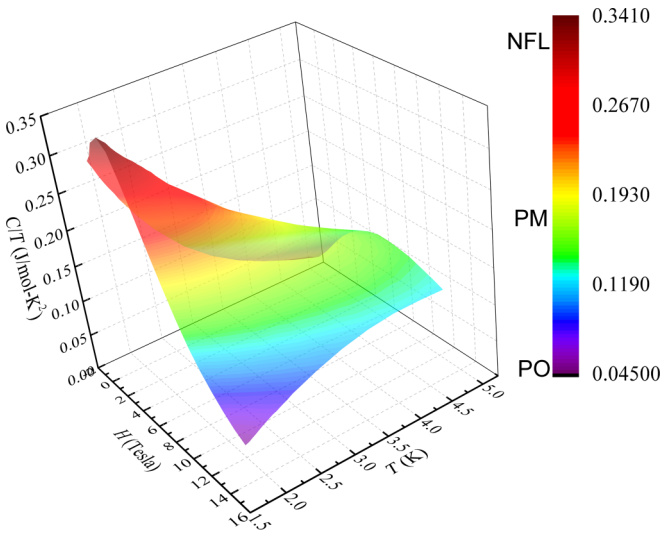

FIG. 7. *H-T* phase diagram extracted from the temperature-dependent heat capacity at different fields for $Ce_{0.24}La_{0.76}Ge$. This diagram indicates three phases: (1) NFL state with short-range correlations, (2) PM phase, and (3) PO associated with the biquadratic exchange couplings.

around $T^* \pm 1$ [above $2(10^4)$ Oe] (see Fig. S3 of the Supplemental Material). Hence, in this compound, it is expected that the biquadratic exchange coupling arises due to spatial magnetic fluctuations, the origin of which is completely different from the reported higher-order magnetization in CeGe.

In addition, from the temperature-dependent heat capacity at different fields (Fig. 3 of Supplemental Material [41]), the possible phases present in $Ce_{0.24}La_{0.76}Ge$ are extracted, as shown in the *H-T* phase diagram (Fig. 7). This compound has three phases; phase I: NFL state, phase II: paramagnetic (PM) phase, and phase III):partial ordering (PO) associated with biquadratic exchange coupling. Generally, the Fermi liquid state is formed in the presence of external parameters (like magnetic fields, pressure, etc.) due to the recovery of the quasiparticle picture. But in $Ce_{0.24}La_{0.76}Ge$, an opposite effect is noted which indicates a relationship between NFL state, magnetic fluctuations, and biquadratic exchange coupling. The observed opposite effect is possibly due to the developing spatial magnetic fluctuations with magnetic fields, which develop the biquadratic exchange coupling.

V. SUMMARY

To summarize, our combined theoretical and experimental study for $Ce_{0.24}La_{0.76}Ge$ compound indicates that, in zero field, there is a presence of local moment fluctuations in the NFL state. In the presence of magnetic fields, local moments interact spatially through conduction electrons and result in the development of biquadratic exchange coupling. This exchange coupling is responsible for the appearance of a partial order parameter in heat capacity. The biquadratic exchange coupling is derived from spatial magnetic quantum fluctuations. Our work highlights the fact that the local moments in the NFL state may participate in the development of the high-order exchange coupling rather than bilinear exchange couplings or Fermi liquid behavior. This implies an interesting ground state in $Ce_{0.24}La_{0.76}Ge$ which is not in accordance with the proposed Doniach model for other Ce-based compounds. Hence, this work might lead to further microscopic experimental studies to investigate the connectivity between the NFL state and biquadratic exchange coupling.

ACKNOWLEDGMENT

The authors acknowledge IIT Mandi for experimental and computational facilities and financial support.

[1] G. R. Stewart, Rev. Mod. Phys. **56**, 755 (1984); **73**, 797 (2001).
[2] P. Gegenwart, Q. Si, and F. Steglich, Nat. Phys. **4**, 186 (2008).
[3] D. R. Grempel and M. J. Rozenberg, Phys. Rev. B **60**, 4702 (1999).
[4] J. Paglione, M. A. Tanatar, D. G. Hawthorn, E. Boaknin, R. W. Hill, F. Ronning, M. Sutherland, L. Taillefer, C. Petrovic, and P. C. Canfield, Phys. Rev. Lett. **91**, 246405 (2003).
[5] H. v. Lohneysen, T. Pietrus, G. Portisch, H. G. Schlager, A. Schroder, M. Sieck, and T. Trappmann, Phys. Rev. Lett. **72**, 3262 (1994).
[6] Y. Tabata, D. R. Grempel, M. Ocio, T. Taniguchi, and Y. Miyako, Phys. Rev. Lett. **86**, 524 (2001).
[7] O. Trovarelli, C. Geibel, S. Mederle, C. Langhammer, F. M. Grosche, P. Gegenwart, M. Lang, G. Sparn, and F. Steglich, Phys. Rev. Lett. **85**, 626 (2000).
[8] M. C. Aronson, R. Osborn, R. A. Robinson, J. W. Lynn, R. Chau, C. L. Seaman, and M. B. Maple, Phys. Rev. Lett. **75**, 725 (1995).
[9] M. Nicklas, M. Brando, G. Knebel, F. Mayr, W. Trinkl, and A. Loidl, Phys. Rev. Lett. **82**, 4268 (1999).
[10] D. L. Cox, Phys. Rev. Lett. **59**, 1240 (1987).
[11] E. Miranda, V. Dobrosavljević, and G. Kotliar, J. Phys.: Condens. Matter **8**, 9871 (1996).
[12] E. Miranda and V. Dobrosavljević, Rep. Prog. Phys. **68**, 2337 (2005).
[13] P. Coleman, *Introduction to Many-Body Physics* (Cambridge University Press, Cambridge, 2015), pp. 660–661.
[14] M. Szlawska and D. Kaczorowski, J. Phys.: Condens. Matter **26**, 016004 (2014).
[15] S. Nakatsuji, S. Yeo, L. Balicas, Z. Fisk, P. Schlottmann, P. G. Pagliuso, N. O. Moreno, J. L. Sarrao, and J. D. Thompson, Phys. Rev. Lett. **89**, 106402 (2002).
[16] J. C. Slonczewski, Phys. Rev. Lett. **67**, 3172 (1991).
[17] V. K. Vlasko-Vlasov, U. Welp, J. S. Jiang, D. J. Miller, G. W. Crabtree, and S. D. Bader, Phys. Rev. Lett. **86**, 4386 (2001).
[18] B. Barbara, A. P. Malozemoff, and Y. Imry, Phys. Rev. Lett. **47**, 1852 (1981).
[19] L. Huang and B. Ao, Phys. Rev. B **87**, 165139 (2013).
[20] P. Werner, E. Gull, M. Troyer, and A. J. Millis, Phys. Rev. Lett. **101**, 166405 (2008).
[21] R. H. McKenzie and D. Scarratt, Phys. Rev. B **54**, R12709 (1996).

[22] L. Huang and H. Lu, Phys. Rev. B **99**, 045122 (2019).
[23] H. Lu and L. Huang, Phys. Rev. B **98**, 195102 (2018).
[24] K. Singh and K. Mukherjee, Europhys. Lett. **126**, 57005 (2019).
[25] K. Singh and K. Mukherjee, Sci. Rep. **9**, 5131 (2019).
[26] C. R. S. Haines, N. Marcano, R. P. Smith, I. Aviani, J. I. Espeso, J. C. Gomez Sal, and S. S. Saxena, Low Temp. Phys. **38**, 651 (2012).
[27] N. Marcano, J. I. Espeso, D. R. Noakes, G. M. Kalvius, and J. C. Gomez Sal, Physica B **359**, 269 (2005).
[28] P. K. Das, N. Kumar, R. Kulkarni, S. K. Dhar, and A. Thamizhavel, J. Phys.: Condens. Matter **24**, 146003 (2012).
[29] T. Jonsson, P. Svedlindh, and M. F. Hansen, Phys. Rev. Lett. **81**, 3976 (1998).
[30] D. C. Johnston, Phys. Rev. Lett. **62**, 957 (1989).
[31] B. Martinez, A. Labarta, R. Rodriguez-Sola, and X. Obradors, Phys. Rev. B **50**, 15779 (1994).
[32] K. Haule, C.-H. Yee, and K. Kim, Phys. Rev. B **81**, 195107 (2010).
[33] A. Georges, G. Kotliar, W. Krauth, and M. J. Rozenberg, Rev. Mod. Phys. **68**, 13 (1996).
[34] P. Blaha, K. Schwarz, F. Tran, R. Laskowski, G. K. H. Madsen, and L. D. Marks, J. Chem. Phys. **152**, 074101 (2020).
[35] J. P. Perdew and Y. Wang, Phys. Rev. B **45**, 13244 (1992).
[36] K. Haule, Phys. Rev. B **75**, 155113 (2007).
[37] K. Haul, Phys. Rev. Lett. **115**, 196403 (2015).
[38] M. Jarrell and J. E. Gubernatis, Phys. Rep. **269**, 133 (1996).
[39] L. Nordheim, Ann. Phys. (Leipzig) **401**, 607 (1931).
[40] M. J. P. Gingras, C. V. Stager, N. P. Raju, B. D. Gaulin, and J. E. Greedan, Phys. Rev. Lett. **78**, 947 (1997).
[41] See Supplemental Material at http://link.aps.org/supplemental/10.1103/PhysRevB.102.235137 for magnetization measurements, heat capacity, impurity hybridization function, effective mass, and crystal structure.
[42] K. Singh and K. Mukherjee, Philos. Mag. **99**, 386 (2019).
[43] J. Lago, S. J. Blundell, A. Eguia, M. Jansen, and T. Rojo, Phys. Rev. B **86**, 064412 (2012).
[44] L. P. Levy and A. T. Ogielski, Phys. Rev. Lett. **57**, 3288 (1986).
[45] H.-D. Kim, O. Tjernberg, G. Chiaia, H. Kumigashira, T. Takahashi, L. Duo, O. Sakai, M. Kasaya, and I. Lindau, Phys. Rev. B **56**, 1620 (1997).
[46] Z. Qian and G. Vignale, Phys. Rev. B **71**, 075112 (2005).
[47] M. Imada, A. Fujimori, and Y. Tokura, Rev. Mod. Phys. **70**, 1039 (1998).
[48] S. A. Shaheen, Phys. Rev. B **36**, 5472 (1987).
[49] C. K. Barman, P. Singh, D. D. Johnson, and A. Alam, Phys. Rev. Lett. **122**, 076401 (2019).
[50] M. Loewenhaupt and M. Prager, Z. Phys. B **62**, 195 (1986).
[51] A. Koitzsch, N. Heming, M. Knupfer, B. Buchner, P. Y. Portnichenko, A. V. Dukhnenko, N. Y. Shitsevalova, V. B. Filipov, L. L. Lev, V. N. Strocov, J. Ollivier, and D. S. Inosov, Nat. Commun. **7**, 10876 (2016).
[52] T. Senthil, Phys. Rev. B **78**, 035103 (2008).
[53] C. Pfleiderer, D. Reznik, L. Pintschovius, H. v. Lohneysen, M. Garst, and A. Rosch, Nature (London) **427**, 227 (2004).
[54] A. J. Kim, H. O. Jeschke, P. Werner, and R. Valenti, Phys. Rev. Lett. **118**, 086401 (2017).
[55] A. I. Lichtenstein, M. I. Katsnelson, and G., and Kotliar, Phys. Rev. Lett. **87**, 067205 (2001).
[56] S. V. Streltsov, E. Gull, A. O. Shorikov, M. Troyer, V. I. Anisimov, and P. Werner, Phys. Rev. B **85**, 195109 (2012).
[57] R. Rieddel, *Handbook of Ceramic Hard Materials* (Wiley, New York, 1989), Chap. 1, p. 11.
[58] R. Shiina, H. Shiba, and P. Thalmeier, J. Magn. Magn. Mater. **177**, 303 (1998).
[59] C. Luo, T. Datta, and D.-X. Yao, Phys. Rev. B **93**, 235148 (2016).
[60] R. Yu and Q. Si, Phys. Rev. Lett. **115**, 116401 (2015).
[61] A. P. Ramirez, P. Coleman, P. Chandra, E. Bruck, A. A. Menovsky, Z. Fisk, and E. Bucher, Phys. Rev. Lett. **68**, 2680 (1992).
[62] S. Sachdev and J. Ye, Phys. Rev. Lett. **70**, 3339 (1993).
[63] P. Werner, A. J. Kim, and S. Hoshino, Europhys. Lett. **124**, 57002 (2018).